Available online at www.sciencedirect.com
SCIENCE DIRECT
ELSEVIER
International Journal of Thermal Sciences 44 (2005) 986–999
International Journal of Thermal Sciences
www.elsevier.com/locate/ijts

A model-based online fault detection and diagnosis strategy for centrifugal chiller systems

Jingtan Cui, Shengwei Wang *

Department of Building Services Engineering, The Hong Kong Polytechnic University, Hong Kong

Received 15 November 2004; received in revised form 7 March 2005; accepted 7 March 2005

Available online 21 April 2005

Abstract

The paper presents an online adaptive strategy for the fault detection and diagnosis of centrifugal chiller systems. The strategy is developed based on six physical performance indexes. These performance indexes have the capability to describe the health condition of centrifugal chillers and particularly to account for existing chiller faults. A set of rules for faults and their impacts on the six performance indexes are deduced from theoretical analysis, and then serve as the fault classifier. The benchmarks of the performance indexes are provided by simplified reference models, whose parameter identification is simple. In addition, an online adaptive scheme is developed, by analyzing uncertainty coming from both model-fitting errors and measurement errors, to estimate and update the thresholds for detecting abnormal performance indexes. The FDD strategy is validated by both field data collected from a real building chiller system and by laboratory data provided by an ASHRAE research project.

Keywords: Fault detection; Fault diagnosis; Centrifugal chiller; Model; Threshold

1. Introduction

Fault detection and diagnosis (FDD) are important in process engineering and have attracted a lot of attention recently. The main benefits of FDD in HVAC&R (Heating, Ventilating, Air-Conditioning and Refrigeration) applications derive from reduced operating costs and/or improved indoor environment. Detailed literature reviews in this field can be found in the papers of Comstock et al. [1], Reddy et al. [2] as well as Dexter and Pakanen [3].

Chiller systems account for a large portion of the energy consumption of HVAC&R system of buildings. It is estimated that energy consumption of chiller plants typically contribute to 35–40% of the total building electricity consumption in commercial buildings in Hong Kong. Furthermore, chiller performance degrades naturally and different kinds of faults (component faults and sensor faults) may occur in the course of operation, which might result in a great waste of energy. As for sensor faults in chiller systems, a series of comprehensive investigations can be found in the works of Wang and Wang [4,5], and Wang and Xiao [6]. Component hard faults which cause the system to stop functioning (e.g., seized compressors, broken fan belts and malfunctioning electrical components) are usually easier to detect, since they occur abruptly and result in a sudden failure of some part of the plant [7]. Component soft faults which cause degradation in system performance (e.g., the fouling of tubes of condensers and evaporators) are the prime concern in this paper.

The fault detection and diagnosis methods might be classified into two major groups [8], including model-free FDD methods, which do not utilize an explicit mathematical model of the target system, and model-based FDD methods, which employ a mathematical model. However, we should confess that there is no clear boundary between these two definitions and sometimes these two methodologies are used

* Corresponding author. Shengwei Wang is an associate professor and the associate head of the Department of Building Services Engineering, The Hong Kong Polytechnic University, Kowloon, Hong Kong. Tel.: +852 27665858; Fax: +852 27746146.

E-mail address: beswwang@polyu.edu.hk (S. Wang).

1290-0729/$ – see front matter
doi:10.1016/j.ijthermalsci.2005.03.004

Nomenclature

$b_0, \ldots, b_7$	regression coefficients in reference models	
COP	coefficient of performance	
C_{pw}	water specific heat	$\mathrm{kJ \cdot kg^{-1} \cdot K^{-1}}$
Eff_{isen}	isentropic efficiency	
Eff_{motor}	motor efficiency	
f_i	reference model of the ith performance index	
$F_i(\cdot)$	error propagation function	
g_i	formula for calculating the ith performance index	
h_{dis}	refrigerant specific enthalpy at compressor discharge	$\mathrm{kJ \cdot kg^{-1}}$
h_{suc}	refrigerant specific enthalpy at compressor suction	$\mathrm{kJ \cdot kg^{-1}}$
$LMTD$	logarithm mean temperature difference	°C
n	number of training data set for regression model fitting	
M_{chw}	chilled water mass flow rate	$\mathrm{kg \cdot s^{-1}}$
M_{cw}	entering condenser water mass flow rate	$\mathrm{kg \cdot s^{-1}}$
M_{ref}	refrigerant mass flow rate	$\mathrm{kg \cdot s^{-1}}$
p	number of independent variables in reference models	
P	pressure	Pa
q_0	specific refrigeration output	$\mathrm{kJ \cdot kg^{-1}}$
Q_{ev}	cooling load	kW
r_i	residual of the ith performance index	
R^2	coefficient of determination	
t	student's distribution	
T	temperature	°C
$Th_{0,i}$	threshold of the ith performance index	
$U(\cdot)$	uncertainty	
v	specific volume	$\mathrm{m^3 \cdot kg^{-1}}$
w_{fit}	model fitting error	
w_{mea}	measurement error	
W_{elec}	electricity consumed by the motor	kW
$\mathbf{X}_0$	vector of independent variables where uncertainty is calculated	
$\mathbf{X}_{\mathrm{reg}}$	matrix of independent variables used in regression models	
Y	response variable of regression model	
$\mathbf{Z}$	vector of true values of measured variables	

Greek symbols

α	fractile
γ	mean isentropic coefficient
ε	random error of regression
σ	standard deviation
δ	Gaussian noise of measured variable

Subscripts

chw	chilled water
cd	condenser
chws	chilled water supply
chwr	chilled water return
cw	condenser water
ecw	entering condenser water
ev	evaporator
i	ith performance index
j	jth element of measurement vector $\mathbf{Z}$
lcw	leave condenser water

Superscripts

$\widehat{\ }$	measured value
$\sim$	estimated value

together. Although a model-free method has a simple structure and the ability to detect and diagnose faults simultaneously, it is difficult to get robust rules and evaluate faults quantitatively.

As for model-based methods, one of the fundamental issues is to identify, as quickly as possible, an accurate reference model of system performance, representing its fault-free behaviour. Model-based FDD methods can be categorized, in terms of the construction of reference models, as follows:

(1) Data driven models (Rossi and Braun [9], Bailey [10], etc.), which do not incorporate any knowledge of the system.
(2) Physical models (Gordon and Ng [11], Bourdouxhe et al. [12], Mclntosh and Mitchell [13], etc.), which are largely based on first principles.
(3) Semi-physical models may be partly data driven and partly based on first principles [7]. Actually, these models are data driven models calibrated by experiments, e.g., CoolTools/ DOE-2 Model [14].

Traditional FDD methods in HVAC&R usually require a great number of measurements as fault indicators (Stylianou and Nikanpour [15], Rossi and Braun [9]). The fault classifiers of the methods use the statistically significant deviations of the measurements to detect a fault and use their deviation pattern to diagnose the fault. Nevertheless it is not an easy job to determine how many and which measurements should be chosen to fulfill this duty as there are numerous sensors available on centrifugal chiller systems. A robust fault classifier in FDD should make use of the impacts of faults on performance indexes with physical meanings rather than on pure numerical values of measurements. Another fundamental issue in FDD applications is to set an appropriate threshold for fault detection. The threshold is usually determined empirically or experimentally. A lower threshold can benefit the earlier detection of major faults but tends to produce false alarms, and vice versa.

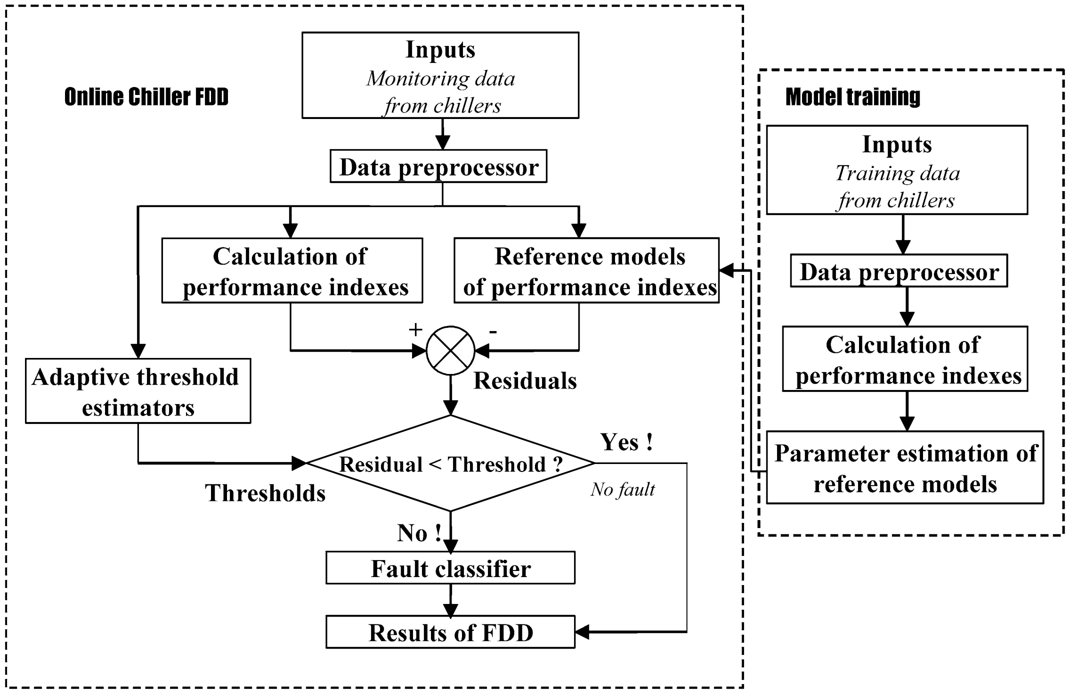

Fig. 1. Schematic diagram of FDD strategy.

The FDD strategy presented in this paper is based on a fault classifier relating six performance indexes that have great thermodynamic meaning to typical chiller faults, instead of relating a great number of measurements to these faults as most previous works did in the chiller FDD field. Moreover, the FDD strategy employs a simple model which is easy to identify to predict normal values of the performance indexes. In order to avoid false alarms and effectively detect a fault, a scheme that can set reasonable fault detection thresholds is developed. The strategy is validated both by field chiller data from the BMS (Building Management System) of a commercial building in Hong Kong and laboratory chiller data provided by the ASHRAE research project 1043-RP (Comstock and Braun [16]).

2. Basic method and approach of strategy

The FDD strategy developed in this study comprises a steady-state filter, reference models, online threshold estimators and a fault classifier, as illustrated in Fig. 1. The reference models of performance indexes with the form of $Y_i = f(Q_{\text{ev}}, T_{\text{chws}}, T_{\text{ecw}})$ have three independent variables only, i.e., the cooling load (Q_{ev}), the chilled water supply temperature (T_{chws}) and the entering condenser water temperature (T_{ecw}). The reason behind such selection is that the correlations between the performance indexes and these independent variables are very strong. The simple structure of the regression models ensures that their parameters can be conveniently identified. A set of generic rules is derived from theoretical analyses in order to correlate the faults with their impacts on performance indexes. The fault classifier, consisting of this set of rules, could identify the existence of particular chiller faults.

Once a set of data from BMS interfaced with chiller control panels pass through a data preprocessor consisting of a steady-state and an outlier filter, all performance indexes at this sampling instance are calculated. Meanwhile the benchmarks of the performance indexes are also provided by their corresponding reference models. Thus the residual for each performance index is generated by comparing the actually measured value with its benchmark provided by reference models, which are trained beforehand. Each residual is compared with its threshold in the fault detection stage. When the residuals of one or more performance indexes are larger than their thresholds, the chiller system is considered to be faulty. Furthermore the particular faults are diagnosed by the fault classifier according to the amount and direction of the deviation of the performance indexes.

It is worth noting that the thresholds of performance index residuals are updated online according to the uncertainty of the estimated residuals, which is contributed by both model fitting errors (w_{fit}) and measurement errors (w_{mea}), as illustrated by Eq. (1). Where, $Th_{0,i}$ is the threshold of the ith performance index, $\tilde{r}_i$ is the residual of the ith performance index, $U(\cdot)$ is the uncertainty at a certain confidence level which can be estimated by the propagation function $F_i(\cdot)$ of the model fitting errors and measurement errors associated with ith performance index. The detailed procedures are explained in the following subsections:

$$Th_{0,i} = U(\tilde{r}_i) = F_i(w_{\text{fit}}, w_{\text{mea}}) \tag{1}$$

Table 1
Mathematical formulation of performance indexes

Performance indexes	Formulations
Logarithm mean temperature difference of condenser	$LMTD_{\mathrm{ev}} = \frac{T_{\mathrm{chwr}} - T_{\mathrm{chws}}}{\ln(\frac{T_{\mathrm{chwr}} - T_{\mathrm{ev}}}{T_{\mathrm{chws}} - T_{\mathrm{ev}}})}$
Logarithm mean temperature difference of condenser	$LMTD_{\mathrm{cd}} = \frac{T_{\mathrm{lcw}} - T_{\mathrm{ecw}}}{\ln(\frac{T_{\mathrm{lcw}} - T_{\mathrm{cd}}}{T_{\mathrm{ecw}} - T_{\mathrm{cd}}})}$
Mass flow rate of refrigerant	$M_{\mathrm{ref}} = \frac{C_{\mathrm{pw}} M_{\mathrm{chw}} (T_{\mathrm{chwr}} - T_{\mathrm{chws}})}{q_0}$
Compressor isentropic efficiency	$Eff_{\mathrm{isen}} = \frac{\frac{\gamma}{\gamma-1} P_{\mathrm{ev}} v_2 [(P_{\mathrm{cd}}/P_{\mathrm{ev}})^{(\gamma-1)/\gamma} - 1]}{h_{\mathrm{dis}} - h_{\mathrm{suc}}}$
Drive motor efficiency	$Eff_{\mathrm{motor}} = \frac{M_{\mathrm{ref}}(h_{\mathrm{dis}} - h_{\mathrm{suc}})}{W_{\mathrm{elec}}}$
Coefficient of performance	$COP = \frac{C_{\mathrm{pw}} M_{\mathrm{chw}} (T_{\mathrm{chwr}} - T_{\mathrm{chws}})}{W_{\mathrm{elec}}}$

2.1. Performance indexes of centrifugal chillers

Six performance indexes are used by the strategy, which are shown in Table 1. They are selected to be physically meaningful and to able to indicate the health condition of a centrifugal chiller system. By comparing the performance indexes with their expected normal values determined by the reference models, the existence of faults can be detected.

The mathematical formulations of the performance indexes, shown in Table 1, are developed on the basis of a standard refrigeration cycle. Obviously the performance indexes can be calculated directly from measurements available on BMS. In the thermophysical perspective, these performance indexes give a more comprehensive picture of the chiller than that a great number of measurements from sensors do. Although the performance indexes are not independent in a fault sense (see Table 2) and therefore weak in diagnosing multiple faults, the strategy based on the performance indexes is still meaningful in most engineering applications as the chance of multiple faults is low and the diagnosis can be achieved with the support of other means.

2.2. Fault classifier

Once faults are detected based on the deviations of one or more performance indexes from their expectations, it is necessary to find the causes of the faults (fault diagnosis). The performance indexes are selected so that different performance indexes are sensitive to different faults. A fault classifier consisting of rules correlating faults and their impacts on performance indexes is constructed. These rules are deduced from basic thermo-physical principles of chiller systems. The fault diagnostic classifier based on these rules has the advantage of being robust, besides being easily understandable.

The following five typical faults, accounting for a significant part of the service calls made according to the survey conducted by Comstock and Braun [16], were concerned in this study:

- Reduced evaporator water flow.
- Refrigerant leakage.
- Excess oil.
- Condenser fouling.
- Non-condensables in refrigerant.

The rules adopted to correlate the above five faults to their impacts on the six performance indexes are listed in Table 2. Where, "—" indicates that no discernible trend is found in the performance index. The sign "▼" indicates the performance index decreases when the severity of a fault increases. The sign "▲" indicates that the performance index increases when the severity of a fault increases. The sign in the brackets describes the trend when expansive valve is available and functioning well. It is worth pointing out that the expansion valve in the centrifugal chiller tends to compensate for the adverse effects of some faults on the performance indexes and then makes the residuals of them less noticeable. Centrifugal chillers using a fixed orifice as the expansion device would notice earlier and more significant residuals of performance indexes than those using an expansion valve. Hence, this issue should be considered when constructing a fault classifier for chillers with different expansion devices.

The correlations in Table 2 are based on the impacts of the faults on the performance indexes, which are interpreted as follows.

- Reduced evaporate water flow increases the evaporator water temperature difference and therefore higher $LMTD_{\mathrm{ev}}$. Since the expansion valve is attempting to keep it nearly constant, the decreases in evaporator pressure and temperature are slight. Also, a reduced *COP* is expected for this fault although it might not be apparent.
- Refrigerant leakage results in lower M_{ref} and smaller $LMTD_{\mathrm{cd}}$ since a less amount of refrigerant in the system tends to reduce the condenser pressures and condensing temperatures. For a chiller with an expansion valve, the valve is able to compensate for the reduction of refrigerant flow by opening further until it cannot com-

Table 2
Rules in fault diagnostic classifier for centrifugal chillers

Fault type	$LMTD_{\mathrm{ev}}$	$LMTD_{\mathrm{cd}}$	M_{ref}	Eff_{isen}	Eff_{motor}	COP
Reduced evaporator water flow	▲	—	—	—	—	▼
Refrigerant leakage	—	▼	▼(—)	—	—	▼(▲)
Excess oil	—	—	—	—	▼	▼
Condenser fouling	—	▲	▲(—)	—	—	▼
Non-condensables	—	▲	—	▲	—	▼

pensate any more. Due to the smaller $LMTD_{cd}$ and the decrease of throttling effect on the whole refrigeration cycle, a small increase of *COP* can be observed if only the expansion valve is capable of fulfilling its duty well. However, a chiller using a fixed orifice as the expansion device would suffer such penalties as reductions in M_{ref} and *COP*.

- Excess oil simply fills up the compressor cavity and submerges some of the gearing in most cases. The viscous effects caused by the excess oil lead to increased mechanical losses in compressors. Consequently Eff_{motor} decreases. At the same time, *COP* will also decrease due to the increased mechanical losses.
- Condenser fouling results in larger $LMTD_{cd}$ and degradation of *COP* subsequently. The reason is that condenser fouling results in higher condensing temperatures. Similarly, an expansion valve in a chiller tends to compensate for the increase of M_{ref} up to certain level, and the refrigerant flow rate in a chiller with a fixed orifice will be affected (i.e., increase) earlier.
- Non-condensables in refrigerant result in larger calculated $LMTD_{cd}$ because the measured condensing pressures which are used to calculate the condensing temperature increases substantially with the increase of non-condensables in the system. Meanwhile, a higher condensing pressure requires higher isentropic work and hereby higher isentropic efficiency, Eff_{isen}. Also, as expected, the chiller efficiency will decrease because the pressure lift across the compressor becomes higher and requires more electrical power input. Note, if the condensing temperature is measured but not calculated, no significant change will be observed in $LMTD_{cd}$.

2.3. Reference models of performance indexes

Reference models of the proposed performance indexes are used to characterize the fault-free operation of a chiller system under certain operating conditions, i.e., to generate the benchmarks of the performance indexes. Assuming constant water flow rate in evaporator and condenser, chiller performance is primarily a function of three variables, the cooling load and the temperature difference between the entering condenser water and leaving evaporator water [17]. Polynomial regression models which can consider these three variables are naturally given top priority.

In this study, a simple chiller model is presented as shown in Eq. (2). The mean and variance of the error term, ε, are assumed to be 0 and σ^2 respectively (i.e., $\varepsilon \sim N(0,\sigma^2)$) [18].

$$\begin{aligned} Y &= f(Q_{ev}, T_{chws}, T_{ecw}) + \varepsilon \\ &= b_0 + b_1 T_{chws} + b_2 T_{ecw} + b_3 Q_{ev} + b_4 T_{chws} T_{ecw} \\ &\quad + b_5 T_{chws} Q_{ev} + b_6 T_{ecw} Q_{ev} + b_7 Q_{ev}^2 + \varepsilon \end{aligned} \tag{2}$$

The model outputs (Y) are assigned to be the performance indexes of concern (i.e., $LMTD_{ev}$, $LMTD_{cd}$, M_{ref}, Eff_{isen}, Eff_{motor}, *COP*). The model is an expression for chiller performance indexes as a function of the cooling load (Q_{ev}), the chilled water supply temperature (T_{chws}) and the entering condenser water temperature (T_{ecw}). The model's validity will be investigated later in Section 3.2. The coefficients ($b_0, \ldots, b_7$) are assumed to be constant, which can be found by linear regression technique using the performance data obtained from the BMS.

2.4. Online estimation of threshold

Model-based FDD methods rely on the determination whether the residuals of performance indexes exceed fault detection thresholds, which vary with system operating conditions. In fact, the uncertainty of the residuals at a specific operating condition is subject to both the prediction uncertainty of the reference models and the calculation uncertainty of performance indexes. Both prediction uncertainty of the reference models and the uncertainty of performance index calculation are often strongly affected by operating conditions, such as the cooling load and the chilled water and cooling water temperatures. Therefore, thresholds of the residuals of performance indexes vary with operation conditions changes, given certain confidence levels. In this study, adaptable thresholds are used, which are estimated online using the scheme described below.

The online threshold estimation scheme is developed on the basis of evaluating the modeling errors and the propagation of each measurement error through the mathematical formulations of the performance indexes, at a specific operating condition. The threshold ($Th_{0,i}$) for the residual of a performance index (r_i), under certain operating conditions, is estimated online according to its uncertainty ($U(\tilde{r}_i)$) at a certain confidence, as shown in Eq. (3).

$$Th_{0,i} = U(\tilde{r}_i) = t_{\alpha/2,n-p}\tilde{\sigma}_{\tilde{r}_i - r_i} \tag{3}$$

where $Th_{0,i}$ is the threshold of the ith performance index, $\tilde{\sigma}^2_{\tilde{r}_i - r}$ is the estimator of the residual of the ith performance index. The residual (r_i) is the difference between the observed value and model predicted value of the ith performance index. $U(\tilde{r}_i)$ is the uncertainty of the residual at a certain confidence level. $\tilde{\sigma}^2_{\tilde{r}_i - r}$ is determined by Eq. (4) and $t_{\alpha/2,n-p}$ is the value of the t distribution with $n-p$ degrees of freedom at a confidence level of $(1-\alpha)$. n is the number of training data points used in the model regression and p is the number of coefficients estimated from the training data.

$$\tilde{\sigma}^2_{\tilde{r}_i - r_i} = \sum_j \left[\left(\frac{\partial g_i}{\partial z_j} \right) \sigma_{z_j} \right]^2 + \tilde{\sigma}^2_{Y_i} \left[1 + \mathbf{X}_0^{\mathrm{T}} \left(\mathbf{X}_{\mathrm{reg}}^{\mathrm{T}} \mathbf{X}_{\mathrm{reg}} \right) \mathbf{X}_0 \right] \tag{4}$$

where g_i is the formula for calculating the ith performance index. z_j is the jth element in the vector of measured variables ($\mathbf{z}$), which is used to calculate the ith performance index (Y_i). σ_{z_j} is the standard deviations of z_j and $\tilde{\sigma}^2_{Y_i}$ is the estimated variance of the regression error of ith performance index. $\mathbf{X}_0$ is the vector of regressors for the current prediction and $\mathbf{X}_0^{\mathrm{T}}$ is transformed from vector $\mathbf{X}_0$. $\mathbf{X}_{\mathrm{reg}}$ is the matrix of regressors associated with the training data and $\mathbf{X}_{\mathrm{reg}}^{\mathrm{T}}$ is the transformed matrix of $\mathbf{X}_{\mathrm{reg}}$. The deduction of Eq. (4) is provided in the appendix of this paper.

2.5. Other issues concerning FDD application

The proposed FDD strategy can be conveniently integrated with BMSs via a standard software interface. Fig. 2 shows a typical schematic diagram of integration of the FDD application software with a BMS. The FDD software running in a computer in the BMS network retrieves the chiller operating data from the database in the BMS central server station to monitor the operation of the chiller system.

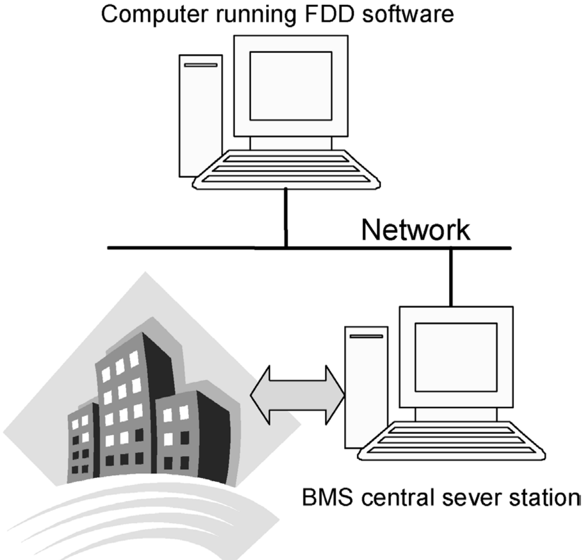

Fig. 2. Schematics of the integration of FDD with BMS.

It is worth pointing out that in addition to identifying the physical cause of faulty operation, e.g., fouled heat exchanger and overridden controls, it is also desirable to estimate both the cost of fixing the fault and the cost of delaying fixing it, which is called fault evaluation. The fault evaluation then balances these two costs and provides appropriate recommendations, including: let it go, adjust the control to compensate for the fault, schedule service when it is convenient, or shut the unit down and repair it now. The procedure of fault evaluation, if considered, would involve much knowledge beyond the scope of HVAC&R engineering itself and it is not concerned in this paper.

3. Validation of FDD strategy using field data

3.1. Chiller system

The data used to validate the proposed strategy were collected from a 1500 ton York seawater cooled centrifugal chiller (using a fixed orifice as the expansive device) in the central cooling system of a commercial building in Hong Kong, over a period of one month. Chilled water and cooling water flow rates, temperatures, and compressor power were collected every minute. The condenser of the chiller is

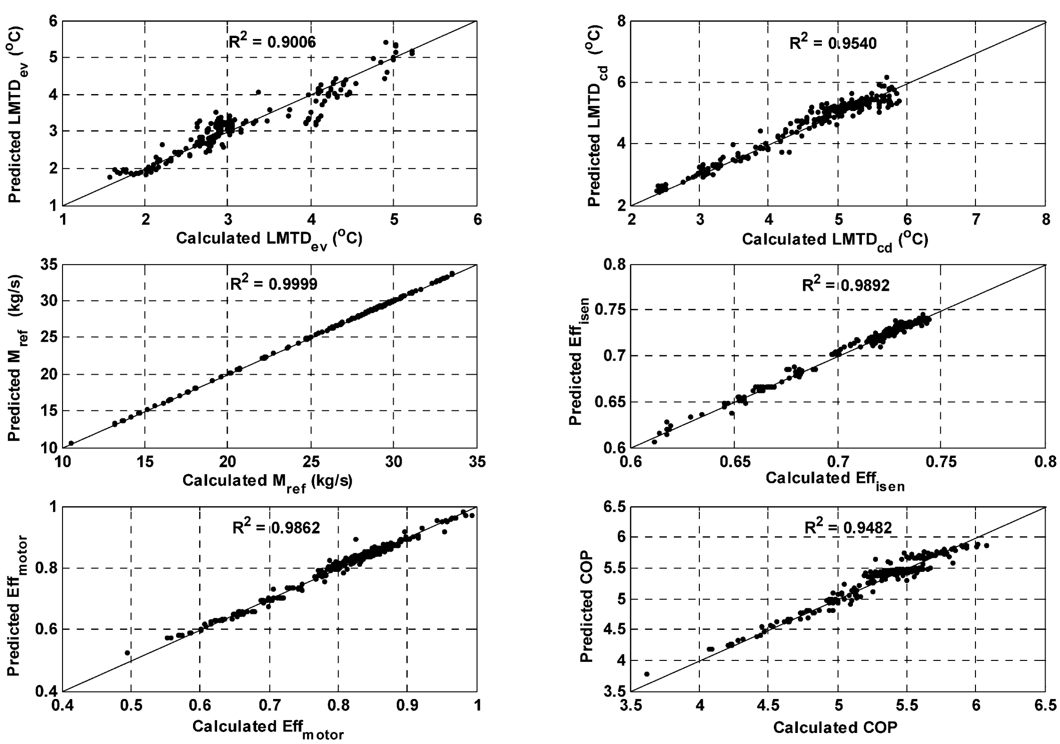

Fig. 3. Comparison between predicted and calculated performance indexes (field data).

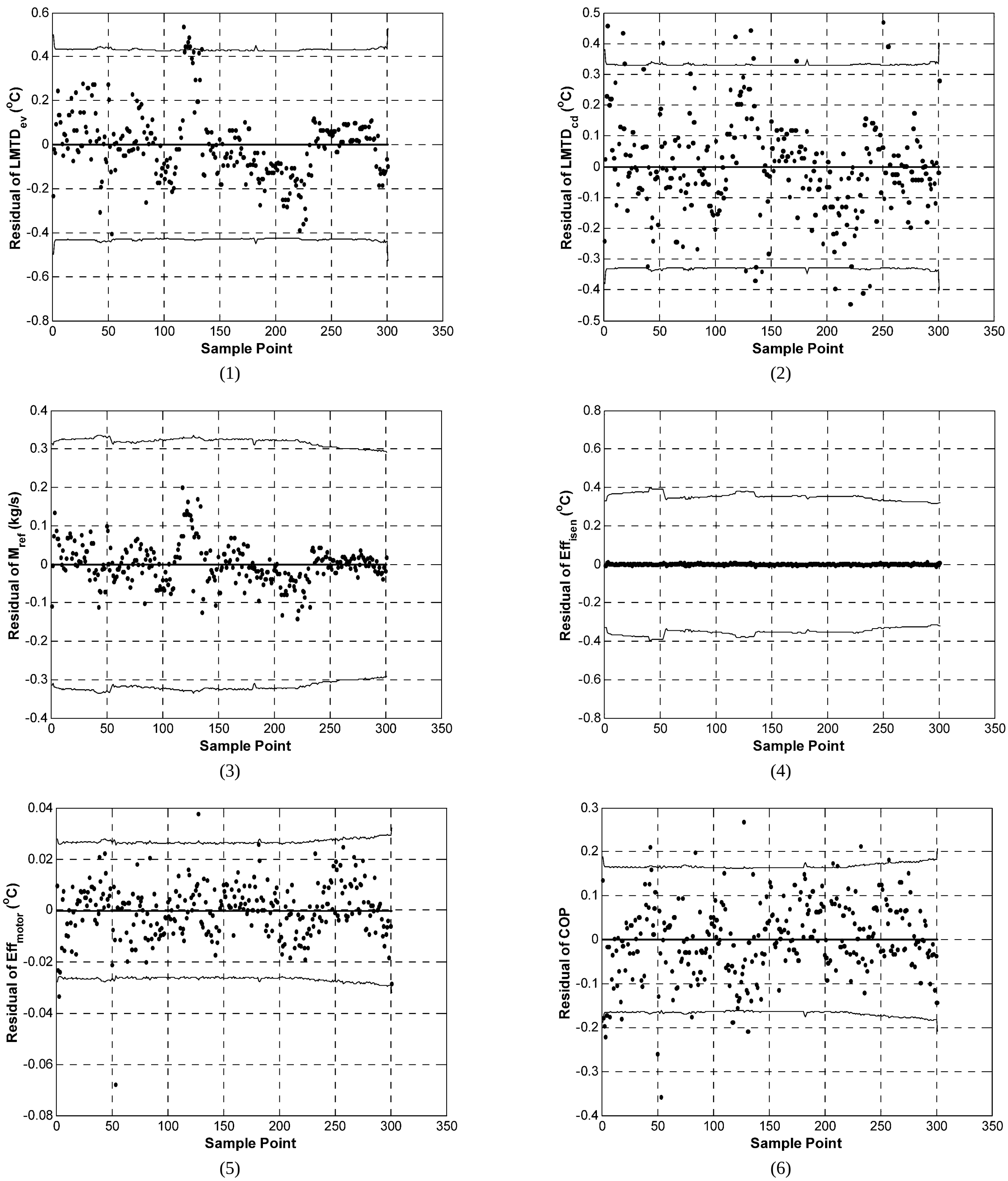

Fig. 4. Normal residuals of performance indexes calculated using field data obtained from 7 : 30 am to 17 : 00 pm on July 5th, 2001: (1) Residuals of $LMTD_{\mathrm{ev}}$; (2) Residuals of $LMTD_{\mathrm{cd}}$; (3) Residuals of M_{ref}; (4) Residuals of Eff_{isen}; (5) Residuals of Eff_{mottor}; (6) Residuals of *COP*.

directly cooled by seawater and the water flow rates through the condenser and evaporator are constant.

3.2. Validation of reference models

In this study, the field-monitored chiller data collected on July 4th, 2001 were used to identify the reference models. The sampling interval was one minute. Since the cooling plant just went through a routine process of re-commissioning, healthy and fault-free operations of the components, sensors, controller, actuator, etc., can be ensured. The collected data sets could therefore be thought to have the capability to describe the fault-free operation of the plant. The noise errors associated with individual measured data were assumed to be Gaussian distribution with mean zero and standard deviation (i.e., half of the measurement accuracy).

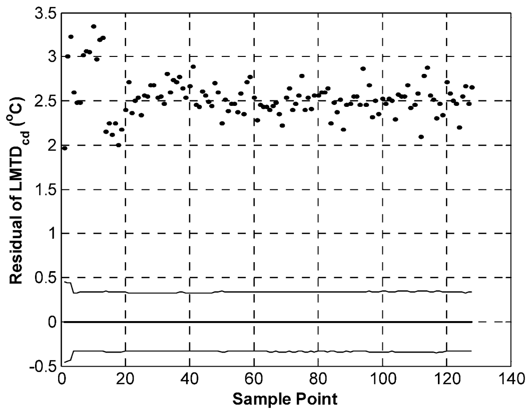

(1)

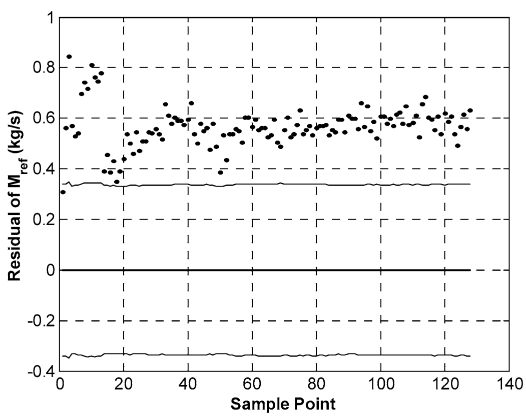

(2)

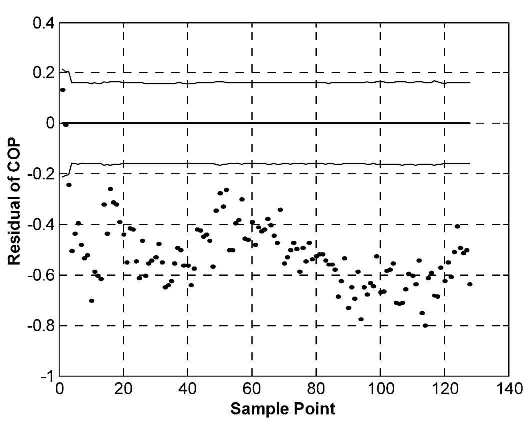

(3)

Fig. 5. Violated residuals of performance indexes calculated using field data obtained from 7:30 am to 17:00 pm on July 31st, 2001: (1) Residuals of $LMTD_{\mathrm{cd}}$; (2) Residuals of M_{ref}; (3) Residuals of COP.

The collected data went through the calibrated steady-state filter first. The training data sets were finally selected prudently from the steady-state data so that the range of variation of the individual variables was as large as possible for identifying sound reference models. OLS (ordinary least square) method was employed to find the parameters of the reference model in the form of Eq. (2). Comparisons between predicted and calculated performance indexes are shown in Fig. 3. R^2 (coefficient of determination) [18] of

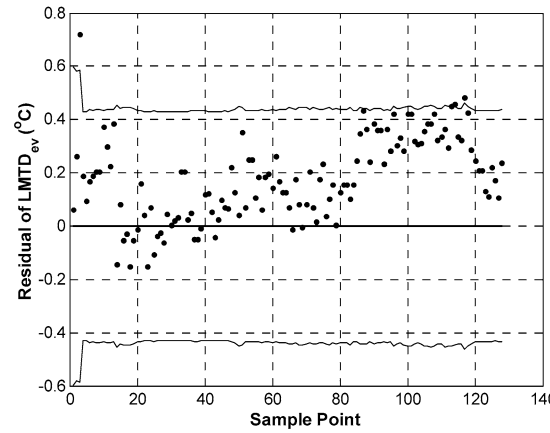

(1)

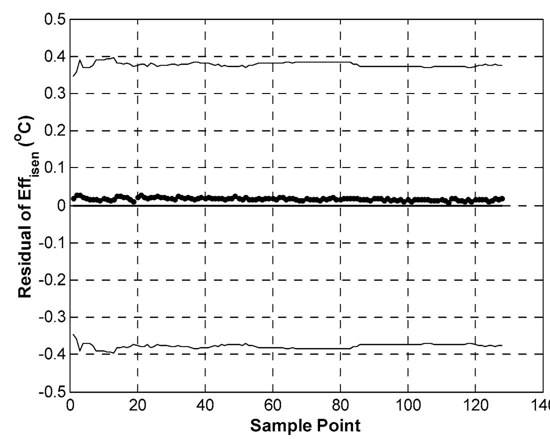

(2)

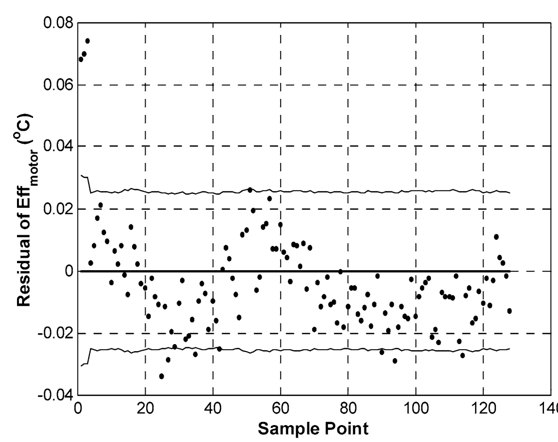

(3)

Fig. 6. Normal residuals of performance indexes calculated using field data obtained from 7:30 am to 17:00 pm on July 31st, 2001: (1) Residuals of $LMTD_{\mathrm{ev}}$; (2) Residuals of Eff_{isen}; (3) Residuals of Eff_{mottor}.

all identified reference models are larger than 90%, which shows the strong goodness-of-fit of the regression models.

3.3. Fault detection and diagnosis using field data

The data of 30 days collected after July 4th, 2001 (the day used for model training) were used to test the performance of the proposed FDD strategy in identifying faulty chiller operation. In the tests, the calculated performance indexes at steady-state were compared with the predictions of corresponding reference models. The variation and size of the residuals were used by the fault classifier to diagnose particular faults. The data collected on July 5th, 2001, which can be regarded as fault free data, were first used in tests. The residuals of the six performance indexes are presented in Fig. 4. The sample points are those samples that passed through the steady-state filter. The dots, "•", in the figures represent the residual values. The solid lines in the figures indicate the threshold band, which is determined by the estimated uncertainty values updated by Eq. (4) with 95% confidence using the measurements. It is evident in the figure that there are a very few residuals locating outside the threshold band. Therefore, it can be concluded that the chiller system is fault free.

Since the condenser of the centrifugal chiller is directly cooled by the seawater, the fouling of the condenser, without purging during the period of 30 days, gradually developed, and naturally degrade the chiller efficiency, *COP*. After July 2th, 2001 (21 days after the commissioning), the FDD strategy started to find significant residuals in $LMTD_{\mathrm{cd}}$, M_{ref} and *COP*, and these residuals gradually became serious. Meanwhile, there was no discernible residual in other three performance indexes. Therefore, the fault classifier concluded that the occurred fault was condenser fouling. This conclusion agreed well with the foregoing expectation that the seawater fouled the condenser and caused an efficiency penalty. The violated residuals of the performance indexes on July 31st, 2001 (28 days after system commissioning and calibration) are presented in Fig. 5. At the same time, the normal residuals of them are also presented in Fig. 6, in which few residuals deviate from their thresholds. Due to constraints in the real system, no other faults were introduced in the chiller system to test the strategy.

4. Validation of FDD strategy using laboratory data from ASHRAE 1043-RP

4.1. Laboratory chiller system

Chiller data from fault tests at different levels of severity are used to validate the FDD strategy developed. The data used were provided by ASHRAE research project 1043-RP [16]. The research project 1043-RP was sponsored by ASHRAE to study faults in chillers and to generate data that can be used in the development and evaluation of FDD methods. The tests were conducted on a 90 ton water-cooled centrifugal chiller with an expansion valve. The cooling load ranged from about 25 to 100% of the rated cooling capacity.

4.2. Validation of reference models

The data from normal tests in the research project were used to train the models. Comparisons between predicted and calculated values of performance indexes are shown in Fig. 7. Also, R^2 of the six identified reference models are all

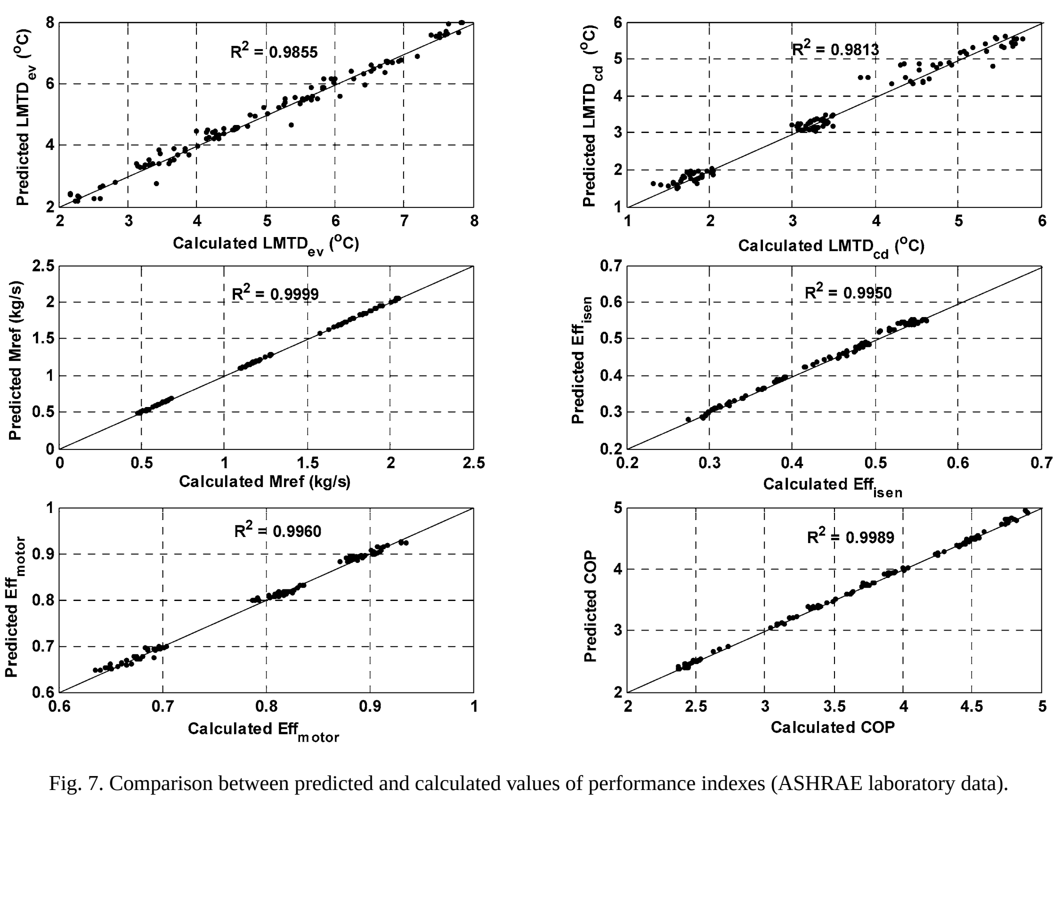

Fig. 7. Comparison between predicted and calculated values of performance indexes (ASHRAE laboratory data).

larger than 98%. That shows desirable goodness-of-fit of the regression models.

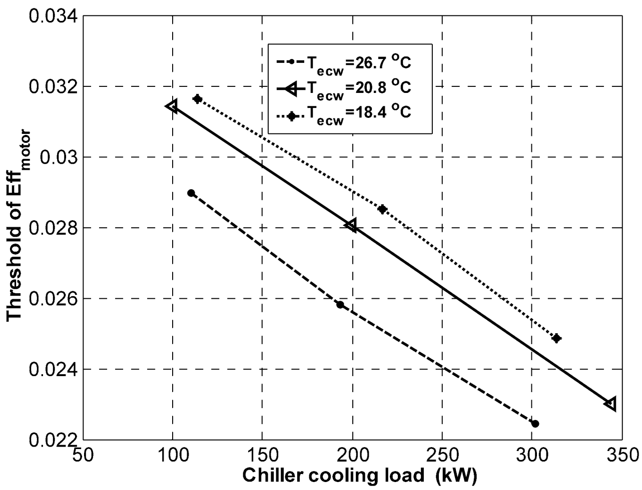

Fig. 8. Estimated threshold of a performance index (Eff_{motor}) affected by chiller cooling load (Q_{ev}) and entering condenser water temperature (T_{ecw}) under the condition of constant chilled water supply temperature (T_{chws}).

4.3. Effects of operating conditions on FDD thresholds

As analyzed earlier in Section 2.4, the chiller operating conditions affect the residual uncertainty of performance indexes, and then affect the thresholds for fault detection at certain fixed confidence level. The laboratory data were used to verify the effects of the operation conditions on the FDD thresholds and check if it is necessary to adopt the online adaptive FDD scheme.

The results show the threshold of each performance index changed with the operating conditions (i.e., cooling load, entering condenser water temperature and chilled supply water temperature). It was observed that the performance indexes, M_{ref}, Eff_{motor}, COP, changed significantly when the operating conditions changed while the performance indexes, $LMTD_{ev}$, $LMTD_{cd}$ and Eff_{isen} were less susceptible to the operating conditions. The threshold of the performance index, Eff_{motor}, was chosen to illustrate such effects. As shown in Fig. 8, the variation of thresholds of Eff_{motor} was significant when the chilling load (Q_{ev}) and the entering condenser water temperature (T_{ecw}) changed at a constant chilled water supply temperature (T_{chws}).

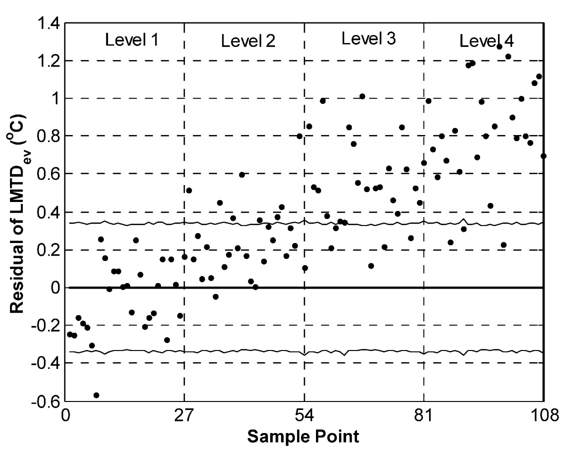

(a)

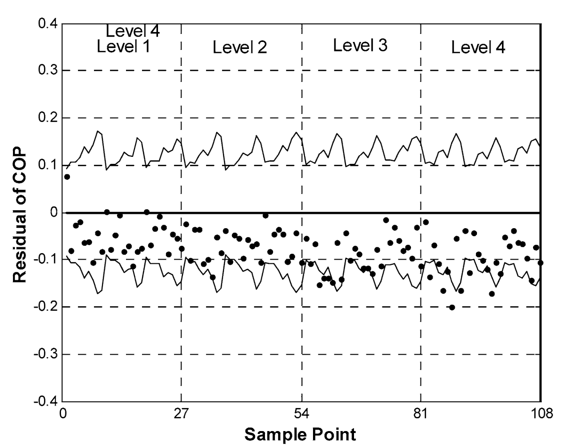

(b)

Fig. 9. Violated residuals of performance indexes obtained during reduced evaporator water flow test: (a) Residuals of $LMTD_{cd}$; (b) Residuals of COP.

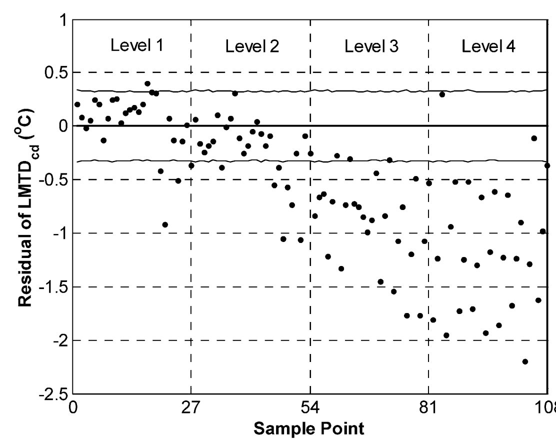

(a)

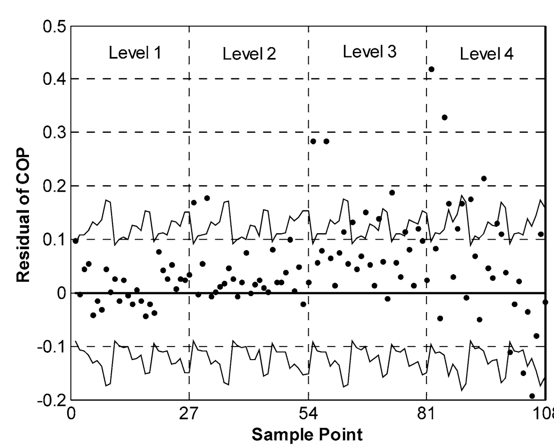

(b)

Fig. 10. Violated residuals of performance indexes obtained during refrigerant leakage test: (a) Residuals of $LMTD_{cd}$; (b) Residuals of COP.

4.4. Fault detection and diagnosis

The data from the tests involving five typical faults were used in this study: reduced evaporator water flow (characterized by reducing water flow), refrigerant leakage (simulated by adding refrigerant to the system); excess oil (simulated by adding oil to the system); condenser fouling (simulated by plugged tubes in the condenser); and non-condensables in refrigerant (simulated by adding nitrogen into the refrigerant). During the validation tests, data of each fault type were arranged in increasing order of severity levels, i.e., from level 1 to level 4, which are defined in by Comstock and Braun [16]. For each fault severity level, there are 27 tests. Thus there are totally 108 (27 × 4) fault tests for each fault type. The residuals of six performance indexes were calculated and then compared with their thresholds at fault detection stage.

In the test of reduced evaporator water flow, the residual of $LMTD_{ev}$ began to deviate beyond its thresholds (here, the confidence level of thresholds is 95%) at fault level 2, as shown in Fig. 9(a). In addition, with the increase fault levels, an ever-decreasing *COP*, though not obvious, could also be observed (Fig. 9(b)). No discernible residual of the rest of the performance indexes was found. These are not presented in this section. The fault classifier, according to the rules presented in Table 2, identified the existence of reduced evaporator water flow.

With regard to the test of refrigerant leakage, the residual of the performance index, $LMTD_{cd}$ (Fig. 10(a)), began to deviate beyond its upper thresholds at fault level 1. In addition, a small increase of *COP* (Fig. 10(b)) was first observed at level 2. Therefore, the refrigerant leakage was identified by the fault classifier considering the chiller is equipped with an expansion valve. In the test of excess oil, only the residuals of Eff_{motor} and *COP* deviated beyond their lower thresholds with increasing fault level, as shown in Fig. 11, while no discernible residual of the other performance indexes was found. The fault classifier identified the existence of excess oil. Similarly, in the case of condenser fouling, as shown in Fig. 12, the residuals of three indexes, $LMTD_{cd}$, M_{ref}, and *COP* deviated from their thresholds. The fault classifier identified the existence of condenser fouling. In the case of non-condensables test, as shown in Fig. 13, the residuals of three indexes, $LMTD_{cd}$, Eff_{isen} and *COP*, deviated from their thresholds. Thus, non-condensable in refrigerant could be identified.

It can also be seen from Fig. 9 to Fig. 13 that the thresholds of the performance indexes, M_{ref}, Eff_{motor}, *COP*, change significantly when the operating conditions change while those of the performance indexes, $LMTD_{ev}$, $LMTD_{cd}$ and Eff_{isen} are less susceptible to the operating conditions. In

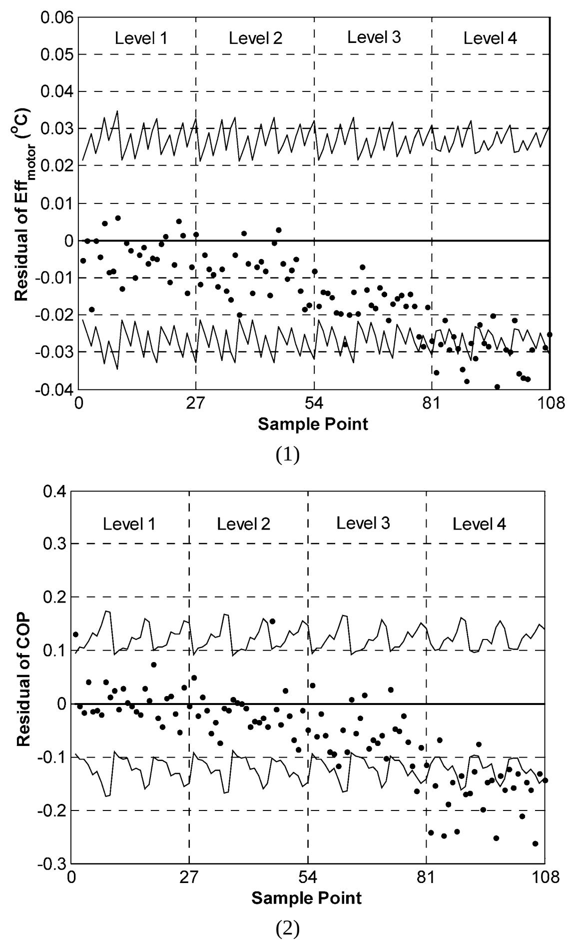

Fig. 11. Violated residuals of performance indexes obtained during excess oil test: (1) Residuals of $LMTD_{motor}$; (2) Residuals of *COP*.

Table 3
Summary of FDD sensitivity and false alarm rate (laboratory data)

Fault type	Reduced evaporator water flow	Refrigerant leakage	Excess oil	Condenser fouling	Non-condensables in refrigerant
Fault level* where a fault is beginning to be detected	Level 2	Level 1	Level 4	Level 1	Level 1
Fault level* where a fault is beginning to be diagnosed	Level 3	Level 2	Level 4	Level 3	Level 1
Detection rate	51%	62%	20%	69%	100%
Diagnosis rate	16%	25%	95%	27%	54%
False alarm rate	1%	4%	1%	1%	1%

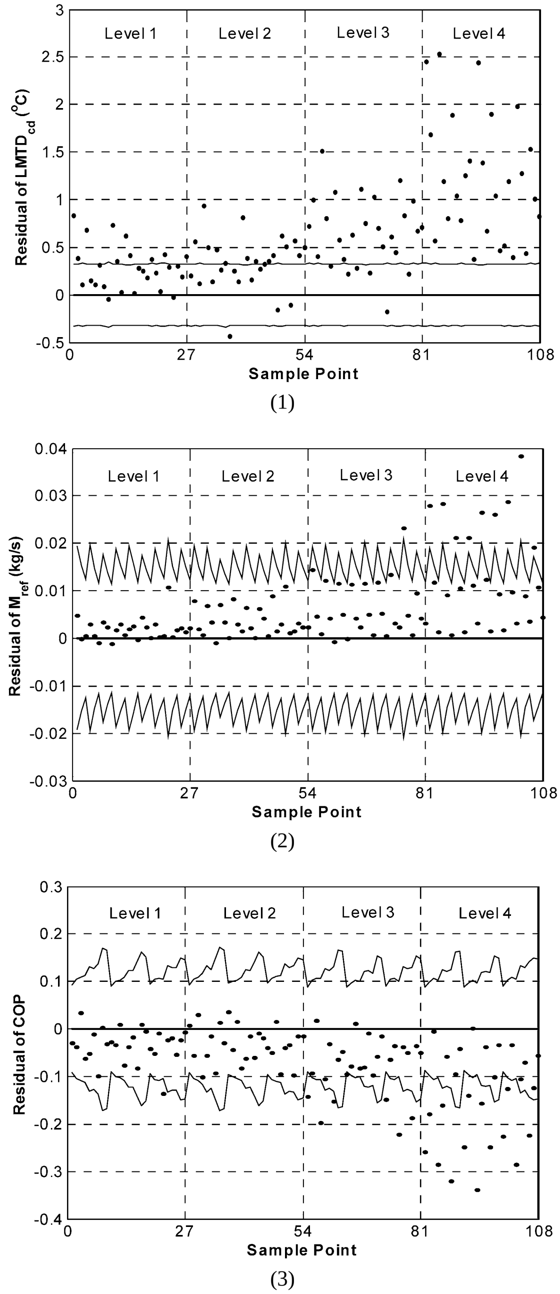

Fig. 12. Violated residuals of performance indexes obtained during condenser fouling test: (1) Residuals of $LMTD_{\mathrm{cd}}$; (2) Residuals of M_{ref}; (3) Residuals of *COP*.

addition, the FDD sensitivity and false alarm rate are summarized in Table 3. The "detection rate" in the table means the ratio of the number of samples which are detected to be faulty to the total number of samples. The "diagnosis rate" is the ratio of the number of samples which are successfully diagnosed to the number of samples which are detected to be faulty. It can be seen from Table 3 that the FDD strategy shows high sensitivity to non-condensables in refrigerant. However the FDD sensitivity to a few faults such as excess oil is not very high. The reason is that excess oil has a strong negative impact on chillers and only a relatively little excess oil was actually introduced to the laboratory centrifugal

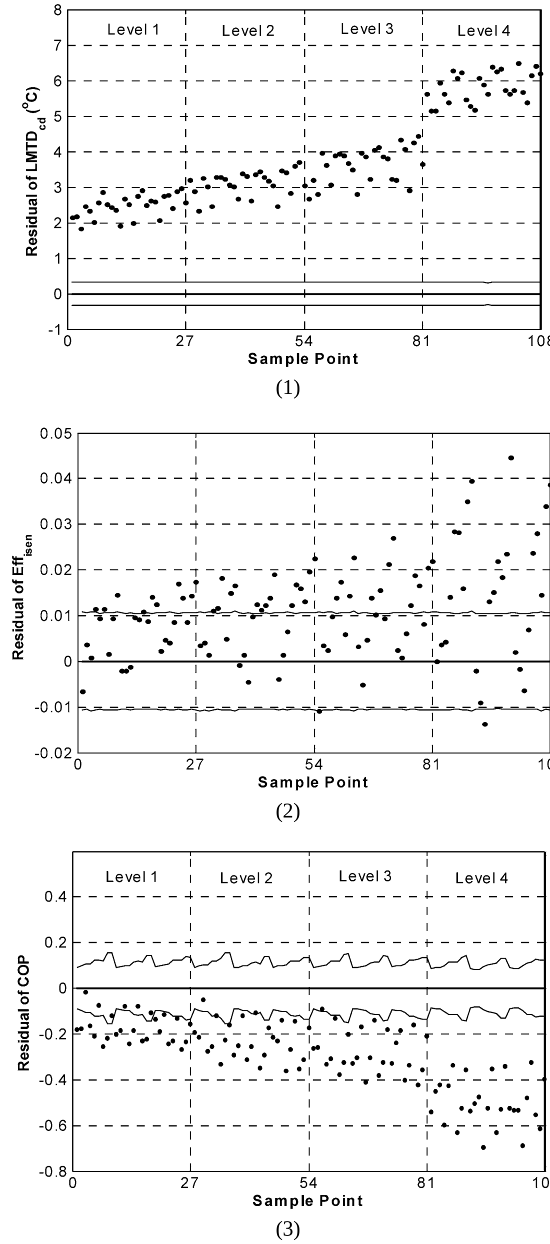

Fig. 13. Violated residuals of performance indexes obtained during non-condensables test: (1) Residuals of $LMTD_{\mathrm{cd}}$; (2) Residuals of Eff_{isen}; (3) Residuals of *COP*.

chiller on the condition that these faults would not do harm to the chiller.

5. Conclusions

The major function of the chiller FDD is to consolidate the information from chillers into a clear and coherent picture of chiller status, which can help building operators detect existing faults and identify the cause of the faults. A model-based FDD strategy with an adaptive fault detection threshold estimator was selected as it is has advantage in model training and online FDD application of centrifugal chillers. The FDD strategy needs no additional instrumentation in implementation and therefore can be easily integrated with existing BMSs.

Validation using both field data and laboratory data show that the FDD strategy, based on a robust classifier and simple reference models, has the capability to detect and diagnose typical chiller faults. Since the reference models provide the baseline behavior of chiller performance, their accuracy and reliability greatly affect online FDD application. During the model identification, it is recommended to select regressor values spreading uniformly over their whole range of variation. The fault classifier for fault diagnosis, deduced from basic physical knowledge, is an effective tool to couple the pattern of the performance indexes with a particular chiller fault. However, it should be confessed that there is no universal fault diagnostic classifier and one needs to be carefully tailored to specific applications. For example, chillers using an expansion valve have a different fault diagnostic classifier from that of chillers using a fixed orifice. In addition, since the set of rules in the fault diagnostic classifier defines qualitatively but not quantitatively the changing trends of the performance indexes when a fault occurs, continuous monitoring of chiller operation is required to help find such trends during the implementation basic chiller FDD.

Due to unavoidable errors associated with both sensor measurements and the model fitting of the reference models, even in the case of fault free operation, there will be residuals between the predicted performance indexes and those which are calculated online. The fault detection threshold defines the acceptable ranges for these residuals and those ranges should be determined quantitatively on the basis of the measurement quality and the fitness of the reference models. In addition, the operating condition of the chiller also has significant effects on the acceptable rage of residuals. The adaptive threshold estimator provides a quantitative approach to scientifically determine thresholds by taking account of these influencing factors.

Acknowledgements

The search presented in this paper was financially supported by a grant of the Research Grants Council (RGC) of the Hong Kong SAR. The authors would like to thank Prof. James Braun, Purdue University, for providing the laboratory data used in this study.

Appendix A. Deduction of Eq. (4)

According to the principle of OLS, the observed value of the ith performance index (Y_i) corresponding to a specific observed regressor vector should satisfy Eq. (A.1).

$$Y_i = f_i\big(\widehat{Q}_{\mathrm{ev}}, \widehat{T}_{\mathrm{ecw}}, \widehat{T}_{\mathrm{chws}}\big) + \varepsilon_i \tag{A.1}$$

where $\widehat{Q}_{\mathrm{ev}}$, $\widehat{T}_{\mathrm{ecw}}$ and $\widehat{T}_{\mathrm{chws}}$ represent the observed (measured) values of Q_{ev}, T_{ecw} and T_{chws}, respectively. ε_i is normally distributed error with a mean of zero and a variance of $\sigma^2_{Y_i}$. $\sigma^2_{Y_i}$ is the variance of the regression error of ith performance index, namely the square of the SEE (standard error of estimate) of Y_i. $f_i(\cdot)$ represents the polynomial regression model of the ith performance index.

Therefore, the normal distribution of Y_i has a mean value of $f(\widehat{Q}, \widehat{T}_{\mathrm{ecw}}, \widehat{T}_{\mathrm{chws}})$ and a variance of $\sigma^2_{Y_i}$, as illustrated by Eq. (A.2).

$$Y_i \sim N\big(f\big(\widehat{Q}, \widehat{T}_{\mathrm{ecw}}, \widehat{T}_{\mathrm{chws}}\big), \sigma^2_{Y_i}\big) \tag{A.2}$$

Also, the output of the corresponding reference model ($\widetilde{Y}_i$) at the same observed regressor vector is normally distributed with a mean value of $f(\widehat{Q}, \widehat{T}_{\mathrm{ecw}}, \widehat{T}_{\mathrm{chws}})$ and a variance of $\sigma^2_{Y_i}\mathbf{X}_0^{\mathrm{T}}(\mathbf{X}_{\mathrm{reg}}^{\mathrm{T}}\mathbf{X}_{\mathrm{reg}})\mathbf{X}_0$ [18]. That can be illustrated by Eq. (A.3).

$$\widetilde{Y}_i \sim N\big(f\big(\widehat{Q}, \widehat{T}_{\mathrm{ecw}}, \widehat{T}_{\mathrm{chws}}\big), \sigma^2_{Y_i}\mathbf{X}_0^{\mathrm{T}}\big(\mathbf{X}_{\mathrm{reg}}^{\mathrm{T}}\mathbf{X}_{\mathrm{reg}}\big)\mathbf{X}_0\big) \tag{A.3}$$

The true value of the residual of the ith performance index, r_i, can be given by Eq. (A.4).

$$r_i = g_i(\mathbf{z}) - Y_i \tag{A.4}$$

where $g_i(\cdot)$ presents the calculation formula of the ith performance index (see Table 3) and $\mathbf{z}$ is the vector of true values of relevant variables.

However, due to measurement and modeling uncertainty, the residual of the ith performance index is estimated as shown in Eq. (A.5).

$$\tilde{r}_i = g_i(\hat{\mathbf{z}}) - \widetilde{Y}_i \tag{A.5}$$

where $\tilde{r}_i$ is the estimate of r_i and $\hat{\mathbf{z}}$ is the vector of measured values of variables considered. $g_i(\hat{\mathbf{z}})$ is the ith performance index calculated using $\hat{\mathbf{z}}$. By replacing $g_i(\hat{\mathbf{z}})$ with $g_i(\mathbf{z})$ plus the first-order item in its Taylor expansion while neglecting the second and higher order, Eq. (A.5) can be further deduced as shown in Eq. (A.6).

$$\tilde{r}_i \approx g_i(\mathbf{z}) + \sum_j \left(\frac{\partial g_i}{\partial z_j}\delta z_j\right) - \widetilde{Y}_i \tag{A.6}$$

where z_j is the jth element in $\mathbf{z}$, δz_j is zero mean Gaussian noise associated with z_j and its standard deviations are σ_{z_j}.

By subtracting Eq. (A.4) from Eq. (A.6), Eq. (A.7) is derived.

$$\tilde{r}_i - r_i = \sum_j \left(\frac{\partial g_i}{\partial z_j}\delta z_j\right) - (\widetilde{Y}_i - Y_i) \tag{A.7}$$

Since δz_j, $\widetilde{Y}_i$ and Y_i are independent of each other [18], the mean and variance of $\tilde{r}_i - r_i$ can be respectively given by Eq. (A.8) and Eq. (A.9) while referring to Eqs. (A.2) and (A.3).

$$E(\tilde{r}_i - r_i) = 0 \tag{A.8}$$

$$D(\tilde{r}_i - r_i) = \sigma^2_{\tilde{r}_i - r_i} = \sum_j \left[\left(\frac{\partial g_i}{\partial z_j}\right)\sigma_{z_j}\right]^2 + \sigma^2_{Y_i}\big[1 + \mathbf{X}_0^{\mathrm{T}}\big(\mathbf{X}_{\mathrm{reg}}^{\mathrm{T}}\mathbf{X}_{\mathrm{reg}}\big)\mathbf{X}_0\big] \tag{A.9}$$

Therefore, $\tilde{r}_i - r_i$ is can been assumed to be normally distributed with mean zero and variance $\sigma_{\tilde{r}_i - r_i}$ as shown in Eq. (A.10).

$$\tilde{r}_i - r_i \sim N\left(0, \sigma^2_{\tilde{r}_i - r_i}\right) \tag{A.10}$$

or,

$$\frac{\tilde{r}_i - r_i}{\sigma_{\tilde{r}_i - r_i}} \sim N(0, 1) \tag{A.11}$$

When $\sigma^2_{Y_i}$ in Eq. (A.9) is replaced with its unbiased estimate, $\tilde{\sigma}^2_{Y_i}$, which is given by Eq. (A.12), the unbiased estimate of $\tilde{\sigma}^2_{\tilde{r}_i - r_i}$ can be obtained by Eq. (A.13).

$$\tilde{\sigma}^2_{Y_i} = \sum_{k=1}^{n} \frac{(Y_k - \widetilde{Y}_k)^2}{n - p} \tag{A.12}$$

$$\tilde{\sigma}^2_{\tilde{r}_i - r_i} = \sum_j \left[\left(\frac{\partial g_i}{\partial z_j}\right)\sigma_{z_j}\right]^2 + \tilde{\sigma}^2_{Y_i}\left[1 + \mathbf{X}_0^{\mathrm{T}}\left(\mathbf{X}_{\mathrm{reg}}^{\mathrm{T}}\mathbf{X}_{\mathrm{reg}}\right)\mathbf{X}_0\right] \tag{A.13}$$

where Y_k is the kth response variable associated with the training data and $\widetilde{Y}_k$ is the output of the reference model. n is the number of training data points used in the model regression and p is the number of coefficients estimated from the training data.

Now, it can be concluded that $\frac{\tilde{r}_i - r_i}{\tilde{\sigma}_{\tilde{r}_i - r_i}}$ has a t distribution with $n - p$ degree of freedom [18] as shown in Eq. (A.14).

$$\frac{\tilde{r}_i - r_i}{\tilde{\sigma}_{\tilde{r}_i - r_i}} \sim t_{n-p} \tag{A.14}$$

This leads to a $(1 - \alpha)$ confidence interval for the predictor of the residual of the ith performance index (r_i), which is shown in Eq. (A.15).

$$\left(\tilde{r}_i - t_{\alpha/2, n-p}\tilde{\sigma}_{\tilde{r}_i - r_i}\right) \leqslant r_i \leqslant \left(\tilde{r}_i + t_{\alpha/2, n-p}\tilde{\sigma}_{\tilde{r}_i - r_i}\right) \tag{A.15}$$

During implementation of FDD, the uncertainty of the predictor of r_i with a $(1 - \alpha)$ confidence level is given in Eq. (A.16).

$$U(\tilde{r}_i) = \pm t_{\alpha/2, n-p}\tilde{\sigma}_{\tilde{r}_i - r_i} \tag{A.16}$$

References

[1] M.C. Comstock, B. Chen, J.E. Braun, Literature review for application of fault detection and diagnostic methods to vapor compression cooling equipment, Ray W. Herrick Laboratories Report HL99-19, Report #4036-2, School of Mechanical Engineering, Purdue University, W. Lafayette, IN, 1999.

[2] T.A. Reddy, D. Niebur, J. Gordon, J. Seem, G. Cabrera, Y. Jia, K.K. Andersen, P. Pericolo, Development and comparison of on-line model training techniques for model-based FDD methods applied to vapor compression chillers: Evaluation of mathematical models and training techniques, Final Report, ASHRAE Research Project 1139, September, 2001.

[3] A. Dexter, J. Pakanen, Fault detection and diagnosis methods in real buildings. International Energy Agency, Energy Conservation in Buildings and Community Systems, Annex 34: Computer-aided evaluation of HVAC system performance, 2001.

[4] S.W. Wang, J.B. Wang, Law-based sensor fault diagnosis and validation for building air-conditioning systems, Internat. J. HVAC&R Res. 5 (1999) 353–378.

[5] S.W. Wang, J.B. Wang, Automatic sensor evaluation in BMS commissioning of building refrigeration systems, Automation in Construction 11 (2002) 59–73.

[6] S.W. Wang, F. Xiao, AHU sensor fault diagnosis using principal component analysis method, Energy and Buildings 36 (2004) 147–160.

[7] P. Haves, Overview of diagnostic method, in: Proceedings of Diagnostics for Commercial Buildings: From Research to Practice, San Francisco, CA, 1999.

[8] J. Gertler, Fault Detection and Diagnosis in Engineering Systems, Marcel Dekker, New York, 1998.

[9] T.M. Rossi, J.E. Braun, A statistical, rule-based fault detection and diagnostic method for vapor compression air conditioners, Internat. J. Heating Ventilating Air Conditioning Refrigerating Res. 3 (1997) 19–37.

[10] M.B. Bailey, The design and viability of a probabilistic fault detection and diagnosis method for vapor compression cycle equipment, PhD thesis, School of Civil Engineering, University of Colorado, 1998.

[11] J. Gordon, K.C. Ng, Centrifugal chillers: thermodynamic modeling and a diagnostic case study, Internat. J. Refrig. 18 (1995) 253–257.

[12] J.P. Bourdouxhe, M. Grodent, J.J. Lebrun, HVAC1 Toolkit: Algorithms and Subroutines for Primary HVAC System Energy Calculations, The American Society of Heating, Refrigerating and Air Conditioning Engineers, 1997.

[13] I.B.D. Mclntosh, J.W. Mitchell, Fault detection and diagnosis in chillers—Part I: Model development and application, ASHRAE Trans. 106 (2000) 268–282.

[14] Pacific Gas and Electric, CoolTools: A Toolkit to Optimize Chilled Water Plants, San Francisco, CA, 2001.

[15] M.P. Stylianou, D. Nikanpour, Performance monitoring, fault detection, and diagnosis of reciprocating chillers, ASHRAE Trans. 102 (1996) 615–627.

[16] M.C. Comstock, J.E. Braun, Fault detection and diagnostic (FDD) requirements and evaluation tools for chillers, ASHRAE 1043-RP, Purdue University, 2002.

[17] J.E. Braun, Methodologies for the design and control of central cooling plant, PhD thesis, University of Wisconsin, Madison, 1988.

[18] D.C. Montgomery, G.C. Runger, Applied Statistics and Probability for Engineers, Wiley, New York, 1994.